

1 **Comparing different computational approaches for detecting long-**
2 **term vertical transmission in host-associated microbiota**

3

4 **Running title: Detecting vertical transmission in microbiota**

5

6 Benoît Perez-Lamarque ^{1,2*} and H el ene Morlon ¹

7

8 ¹ *Institut de biologie de l' cole normale sup rieure (IBENS),  cole normale sup rieure, CNRS,*

9 *INSERM, Universit  PSL, 46 rue d'Ulm, 75 005 Paris, France*

10 ² *Institut de Syst matique,  volution, Biodiversit  (ISYEB), Mus um national d'histoire*

11 *naturelle, CNRS, Sorbonne Universit , EPHE, UA, CP39, 57 rue Cuvier 75 005 Paris, France*

12

13 * *corresponding author: benoit.perez@ens.psl.eu; ORCID: 0000-0001-7112-7197*

14 **Abstract:**

15

16 Long-term vertical transmissions of gut bacteria are thought to be frequent and
17 functionally important in mammals. Several phylogenetic-based approaches have
18 been proposed to detect, among species-rich microbiota, the bacteria that have been
19 vertically transmitted during a host clade radiation. Applied to mammal microbiota,
20 these methods have sometimes led to conflicting results; in addition, how they cope
21 with the slow evolution of markers typically used to characterize bacterial microbiota
22 remains unclear. Here, we use simulations to test the statistical performances of two
23 widely-used global-fit approaches (ParaFit and PACo) and two event-based
24 approaches (ALE and HOME). We find that these approaches have different strengths
25 and weaknesses depending on the amount of variation in the bacterial DNA sequences
26 and are therefore complementary. In particular, we show that ALE performs better
27 when there is a lot of variation in the bacterial DNA sequences, whereas HOME
28 performs better when there is not. Global-fit approaches (ParaFit and PACo) have
29 higher type-I error rates (false positives) but have the advantage to be very fast to run.
30 We apply these methods to the gut microbiota of primates and our results suggest that
31 only a small fraction of their gut bacteria is vertically transmitted.

32

33 **Key words:** metabarcoding, vertical transmission, cophylogeny, microbiota, ecological
34 interactions, primate

35 **Introduction:**

36

37 Most mammals strongly rely on their associated microbial communities, called
38 microbiota, for various functions like their nutrition, protection, or development
39 (Hacquard et al., 2015; McFall-Ngai et al., 2013; Selosse, Baudoin, &
40 Vandenkoornhuyse, 2004). A range of strategies have evolved to ensure the efficient
41 transmission of some microbes across each generation, including direct transmissions
42 at birth, during parental care, or through social contact (Moran, Ochman, & Hammer,
43 2019). If these transmissions are stable and faithful, host-microbe interactions are
44 conserved in the host lineage over long-time scales, and we refer to this process as
45 vertical transmission (following the definition of Groussin et al., 2017). At host
46 speciation, vertically transmitted microbes can be inherited by the two daughter host
47 species and separately evolve as independent strains in each host lineage, resulting in
48 a pattern of cophylogeny, where the tree of microbial strains mirrors the host
49 phylogenetic tree (de Vienne et al., 2013; Page, 1994). Conversely, if a microbe is
50 acquired from the environmental pool of microbes at each host generation and if these
51 microbial pools are not as geographically structured as the host species, we do not
52 expect cophylogenetic patterns between the microbe and the host. Cophylogenetic
53 patterns of vertically transmitted microbes can also be erased by frequent horizontal
54 transfers from particular host lineages to others (*i.e.* host-switches).

55

56 Several studies have reported long-term vertical transmissions among the
57 bacterial gut microbiota of mammals (Gaulke et al., 2018; Groussin et al., 2017; Moeller
58 et al., 2016; Perez-Lamarque & Morlon, 2019; Sanders et al., 2014; Youngblut et al.,
59 2019). Evidence mainly comes from analyses of DNA metabarcoding datasets, where
60 the whole bacterial communities are characterized using the 16S rRNA gene, a short
61 and slowly evolving region (Ochman et al., 2010). A general approach to identifying
62 vertically transmitted bacteria consists in (i) clustering the 16S rRNA sequences into
63 operational taxonomic units (OTUs) based on sequence similarity, (ii) reconstructing
64 for each bacterial OTU a tree of its strains (*i.e.* distinct haplotype sequences), and (iii)
65 inferring which OTUs present a cophylogenetic pattern with the host, which would
66 suggest that the corresponding OTUs are vertically transmitted. This general approach
67 has led to estimates of the proportion of vertically transmitted gut bacteria in
68 mammals ranging from more than 50% of all bacterial OTUs (Groussin et al., 2017) to
69 only 14% (Gaulke et al., 2018), or even as few as ~8% in great apes (Perez-Lamarque &
70 Morlon, 2019). These discrepancies likely come from the use of different approaches
71 to identify cophylogenetic patterns, and from differences in the statistical
72 performances of these different approaches.

73

74 Various approaches have been developed in the past decades to identify
75 cophylogenetic patterns, *i.e.* to assess the congruence between host and symbiont
76 phylogenies (de Vienne et al., 2013; Dismukes, Braga, Hembry, Heath, & Landis, 2022;
77 Legendre, Desdevises, & Bazin, 2002; Page, 1994). These approaches have been applied
78 to a variety of host-symbiont systems and have advanced our understanding of the
79 evolution of such symbiotic interactions (Blasco-Costa, Hayward, Poulin, & Balbuena,
80 2021; Hayward, Poulin, & Nakagawa, 2021). In particular, cophylogenetic approaches
81 have been used to assess whether and how host-symbiont associations impact deep-
82 time evolutionary processes, through vertical transmission and/or preferential host-
83 switches (Blasco-Costa et al., 2021; De Vienne, Giraud, & Shykoff, 2007; de Vienne et
84 al., 2013). A common difficulty of these interpretations is the fact that shared
85 biogeographic structure between hosts and symbionts, for example as a result of
86 vicariance, can also generate cophylogenetic patterns. In particular, if environmental
87 pools of symbionts differ across geographic regions occupied by closely related host
88 species, this can generate cophylogenetic patterns in the absence of vertical
89 transmission (Amato et al., 2019; Perez-Lamarque, Krehenwinkel, Gillespie, & Morlon,
90 2022). Additional precautions are therefore required to link a cophylogenetic pattern
91 to long-term vertical transmission.

92

93 Co-phylogenetic approaches can be divided into two main categories (de
94 Vienne *et al.*, 2013, Table 1). The first category, referred to as ‘global-fit’ approaches,
95 measures a global congruence between the host and symbiont evolutionary histories.
96 For instance, ParaFit (Legendre et al., 2002) and PACo (Balbuena, Míguez-Lozano, &
97 Blasco-Costa, 2013) are two widely used approaches based on the fourth-corner
98 statistic or Procrustes superimposition, respectively. These approaches can be directly
99 applied to the symbiont genetic distances and thus do not require a robust
100 reconstruction of the symbiont phylogenetic tree. They can also handle multiple
101 strains per extant host species. However, they only provide a measure of a
102 cophylogenetic pattern and do not inform on the processes at play. The second
103 category of approaches, referred to as ‘event-based’ approaches, directly models the
104 events of codivergence, host-switches, duplications, and/or losses, to reconcile the
105 host and symbiont phylogenies, while considering the uncertainty in the symbiont
106 evolutionary history (Figure 1). For instance, ALE (Szöllősi, Rosikiewicz, et al., 2013)
107 uses a posterior distribution of symbiont phylogenetic trees to fit reconciliation events.
108 This approach therefore fully models phylogenetic uncertainty in contrast with
109 mainstream event-based approaches using maximum parsimony, e.g. TreeMap (Page,
110 1994) or eMPress (Santichavekin et al., 2021), which are better suited when

111 phylogenetic reconstructions are robust. ALE also accounts for the possibility that the
112 symbiont was absent in the ancestor of all hosts and only secondarily acquired
113 (Szöllősi, Tannier, et al., 2013). It considers unsampled or extinct host lineages and
114 even assumes that host-switching between sampled lineages always involves an
115 unsampled or extinct host lineage as an intermediate (Szöllősi, Tannier, et al., 2013).
116 This is particularly relevant as under-sampling of the extant host species is often
117 important when looking at dynamics of microbial transmission in large animal clades
118 such as mammals (Groussin et al., 2017; Youngblut et al., 2019)). A limitation of ALE
119 is that only uses the information contained in the topology of phylogenetic trees, and
120 sometimes the order of the nodes in the host phylogenetic tree, but not branch lengths
121 (Szöllősi, Tannier, et al., 2013). Another approach (called HOME) was recently
122 developed with the specific aim of analyzing microbiota (meta)barcoding data with
123 little phylogenetic information by avoiding the reconstruction of unreliable trees of
124 OTU strains (Perez-Lamarque & Morlon, 2019). Rather than first reconstructing trees
125 of OTU strains as in ALE, HOME directly models the bacterial DNA substitution
126 process on the host phylogeny under a scenario of vertical transmission with potential
127 host-switches. A limitation of the approach is that it cannot handle multiple OTU
128 strains per extant host, as it does not model duplication events and assumes
129 replacement of the microbial strain rather than coexistence upon host-switch. HOME
130 does not explicitly model potential losses of microbial strains either, nor does it
131 consider unsampled or extinct host lineages. Yet, the direct modeling of DNA
132 evolution offered by HOME can be particularly valuable when the host clade has
133 diverged recently and molecular markers used to characterize the microbiota have
134 accumulated very few substitutions.

135

136 Here, we aim to test the statistical performances of different cophylogenetic
137 approaches to detect vertical transmission in microbiota characterized by
138 metabarcoding techniques. We simulate the evolution of 16S rRNA gene sequences for
139 bacteria that are either vertically transmitted or evolving independently of the host
140 phylogeny. We measure the statistical power (the proportion of vertically transmitted
141 bacteria inferred as being vertically transmitted) and the type-I error rate (the
142 proportion of independently evolving bacteria inferred as being vertically transmitted;
143 *i.e.* false-positives) of ParaFit, PACO, ALE, and HOME. Then, we apply these different
144 methods to the gut bacterial microbiota of 18 new-world and old-world primate
145 species using the dataset generated by Amato et al. (2019). Based on our results, we
146 discuss the pros and cons of each approach and highlight promising areas for future
147 development.

148 **Methods:**

149

150 **Primate phylogeny:**

151

152 In order to design our simulations with realistic settings and to better interpret
153 our empirical analyses of the gut microbiota of primates (Amato *et al.* (2019)), we
154 performed all the simulations on the primate phylogenetic tree of Dos Reis *et al.* (2018).
155 This tree is a nearly complete phylogenetic tree of extant primates (367 species)
156 reconstructed using phylogenomic data and fossil calibrations, with a crown age
157 estimate of ~74 million years (Myr). For computational reasons, we scaled the age of
158 the primate phylogeny to 1 (relative timing) using the R-package ape (Paradis, Claude,
159 & Strimmer, 2004; R Core Team, 2022).

160

161 **Simulations:**

162

163 We simulated three different scenarios of host-microbiota evolution on the
164 complete primate phylogenetic tree (Figure 1): (I) strict vertical transmission where
165 each microbial OTU evolves directly on the host phylogeny (Figure 1b i), (II) vertical
166 transmission with a given number of horizontal host-switches (5, 10, 15, or 20, Figure
167 1b ii), or (III) environmental acquisition, where the microbes evolve independently and
168 are randomly acquired by the extant host species (Figure 1b v). Each simulation
169 generates a tree of OTU strains (Figure 1c). For II (vertical transmission with host-
170 switches), we considered that host-switches can happen uniformly on the host
171 phylogeny from a donor branch to a receiving branch where it replaces the previous
172 OTU strain (Figure 1b ii). The range of simulated horizontal host-switches was chosen
173 to test their effect when they were rare to moderately frequent, as codivergence with
174 very frequent switches can no longer be considered as a scenario of vertical
175 transmission. For III (environmental acquisition), the tree of an independently-
176 evolving OTU was obtained by simulating a pure birth process using the function
177 *pbtree* (R-package ape (Paradis *et al.*, 2004)) until reaching as many tips as primate
178 species; we then randomly assigned each tip in the tree of OTU strains to a primate
179 species, mimicking the process of random strain acquisition from an environmental
180 pool (Figure 1b v).

181

182 For each scenario and each tree of OTU strains, we simulated on this tree the
183 evolution of a 300 bp DNA region mimicking the V4 region of the 16S rRNA gene. We
184 thus obtained for each OTU a DNA alignment made of the DNA sequences from each
185 extant host species. We assumed that 10% of the sites were variable (other sites are

186 kept conserved) and for these variable sites, DNA substitutions were modeled using a
187 K80 process (Kimura, 1980) with different relative substitution rates (μ): 1.5 (many
188 substitutions), 1, 0.5, 0.1, and 0.05 (very few substitutions). These relative rates were
189 chosen to obtain numbers of segregating sites and strains in the simulated alignments
190 that are consistent with the empirical within-OTU alignments: For $\mu=1.5$, we obtained
191 alignments with a mean number of segregating sites >20 and a total number of strains
192 >15 , while for $\mu=0.05$, the simulated alignments had on average <5 segregating sites
193 and <5 number of strains (Supplementary Fig. 1). These simulations were performed
194 using the function *sim_microbiota* in the R-package HOME (Perez-Lamarque & Morlon,
195 2019; R Core Team, 2022).

196

197 Finally, to insert our simulations in the frequently encountered situation when
198 only a small fraction of the extant host species has their microbiota characterized, we
199 retained only the simulated OTU strains present in the 18 primate species sampled in
200 Amato *et al.* (2019). For each OTU, a single OTU strain is associated with each host
201 species. We refer to the corresponding alignments as the ‘simulations without
202 duplications or losses’.

203

204 In addition to the simulations without duplications or losses, we considered
205 that OTU strains can be lost during host evolution or not detected in extant host-
206 associated microbiota using metabarcoding techniques (Figure 1b iii). To mimick this,
207 we randomly sampled, in each alignment, the strains of 10 out of 18 extant host species.
208 We refer to these alignments as the “simulations with losses”. We also considered that
209 intra-host duplications can happen stochastically during host evolution (Figure 1b iv),
210 such that multiple OTU strains can persist in a host lineage. We simulated the same
211 scenarios as above, but simultaneously simulated duplication events using a
212 continuous-time Markov process, *i.e.* duplications can happen at any time on the host
213 branches, with a relative rate $\delta=2$. We obtained alignments by selecting the OTU strains
214 present in each of the 18 primate species. We referred to these alignments as the
215 “simulations with duplications.” Finally, we simulated losses and/or non-detection in
216 the simulations with duplications, by randomly sampling the OTU strains of 10 out of
217 18 extant host species in each alignment. We thus obtained “simulations with losses
218 and duplications”.

219

220 For each simulated scenario and combination of parameters, we performed 100
221 simulations. We therefore obtained a total of 12,000 simulated alignments.

222 **Inferring vertically transmitted OTUs:**

223

224 We considered four different approaches for detecting vertical transmission:
225 two global-fit approaches, ParaFit and PACo, and two event-based approaches, ALE
226 and HOME (Table 1). Other global-fit approaches exist for detecting vertical
227 transmission, like the global-fit approaches proposed by Hommola *et al.* (2009), which
228 is a generalization of the Mantel tests, but we chose to only focus on the two most
229 frequently used ones (ParaFit and PACo: Gaulke *et al.*, 2018; Youngblut *et al.*, 2019).

230

231 Event-based and global-fit approaches rely on the same randomization-based
232 approach to assess statistical significance. After fitting the model under a scenario of
233 vertical transmission (for event-based approaches) or computing the statistic of the test
234 (for global-fit approaches), randomizations are used for generating null expectations
235 under a scenario of independent host-OTU evolution. By comparing the observed fit
236 to null expectations, we may reject the null hypothesis of independent evolution and
237 conclude that the OTU is vertically transmitted. Two different randomization schemes
238 have been used (Table 1). For ParaFit and PACo, Balbuena *et al.* (2013) and Legendre
239 *et al.* (2002) used a randomization scheme that we refer to as *null model 1* (also referred
240 to as “r0” in Hutchinson *et al.* (2017)), which consists in permuting the host species
241 associated to each OTU strain, independently for each strain. The number of host
242 species per OTU strain is therefore maintained, but the number of OTU strains per
243 host species is not, and can even reach 0. For ALE and HOME, a stricter randomization
244 scheme has been used (that we refer to as *null model 2*) that consists in shuffling
245 species names in the host phylogenetic tree, which guarantees that each host species
246 has at least one OTU strain. We used this null model in our ALE and HOME analyses
247 and used it also in addition to *null model 1* for ParaFit and PACo (Table 1). The choice
248 of the number of randomizations used for these tests results from a trade-off between
249 accuracy and computation time. Given the computational requirements of the
250 different approaches (see Results), we used 10,000 randomizations for the global fit
251 approaches (ParaFit and PACo) and 100 for the event-based approaches (ALE and
252 HOME).

253

254 We ran ParaFit and PACo on the phylogenetic distances between pairs of extant
255 primate species and the microbial genetic distances between pairs of OTU strains. We
256 computed these genetic distances using a K80 model of DNA substitution, which
257 corrects for potential mutation saturation. ParaFit and PACo statistics were both
258 computed using a Cailliez correction for negative eigenvalues. We amended the
259 functions *parafit* and *PACo* from the R-packages *ape* (Paradis *et al.*, 2004) and *paco*

260 (Hutchinson, Cagua, Balbuena, Stouffer, & Poisot, 2017) respectively, to avoid
261 technical issues when the number of OTU strains is low. To evaluate the significance
262 of the statistic of each test of vertical transmission, we compared its value to a null
263 distribution under the hypothesis of independent host-OTU evolution using 10,000
264 randomizations, with both *null model 1* and *null model 2*. Balbuena et al. (2013)
265 recommend using 100,000 permutations for high precision; we reduced this number
266 here to save computational time and energy and checked that this did not affect our
267 results on a subset of simulations (see Results). To avoid computational issues during
268 the randomizations of the associations between hosts and OTU strains, we only ran
269 ParaFit and PACo for the alignments containing at least 3 different strains.

270

271 To run ALE, one needs first to generate a posterior distribution of trees of OTU
272 strains using Bayesian phylogenetic inference. We reconstructed phylogenetic trees for
273 each alignment using PhyloBayes (Lartillot & Philippe, 2004) following Groussin *et al.*
274 (2017). We ran PhyloBayes for 4,000 generations, sampling at every generation after an
275 initial burn-in of 1,000 generations. We then ran ALE with the host phylogeny and the
276 distribution of trees of OTU strains as inputs, using the *ALEml* program available at
277 <https://github.com/ssolo/ALE>. ALE estimates the maximum likelihood rates of host-
278 switch, duplication, and loss, and generates a set of host-OTU reconciliations. We used
279 100 reconciliations and computed an average number of codivergences, host-switches,
280 duplications, and losses. To evaluate the significance of these estimated scenarios of
281 vertical transmission, we shuffled the primate species in the phylogenetic tree (*null*
282 *model 2*) and re-ran ALE to obtain a distribution of the number of reconciliation events
283 under a null hypothesis of independent host-OTU evolution. We then compared two
284 criteria to reject the null hypothesis. First, we used the criterium of Groussin *et al.*
285 (2017): (i) the estimated number of codivergences is significantly higher than the
286 number of host-switches and (ii) under a null hypothesis of independent host-OTU
287 evolution, the estimated number of codivergences is higher than the number of host-
288 switches in at most 5% of the null expectations. Second, as in Dorrell *et al.* (2021), we
289 considered that an OTU is vertically transmitted if (i) the estimated number of
290 codivergences is higher than 95% of the null expectations and if (ii) the estimated
291 number of host-switches is lower than 95% of the null expectations. We performed 100
292 randomizations per OTU, except when analyzing simulations with intra-host
293 duplications; in this case, ALE is more computationally intensive and we thus
294 performed only 50 randomizations. We ran ALE only for alignments that had at least
295 one segregating site.

296

297 We ran HOME using the function *HOME_model* in the R-package HOME
298 (Perez-Lamarque & Morlon, 2019). For each alignment, HOME outputs the maximum-
299 likelihood estimates of the number of host-switches and the substitution rate. In
300 HOME, the likelihood is estimated using Monte Carlo simulations (Perez-Lamarque
301 & Morlon); here we used 5,000 simulated trees and picked the tested numbers of host-
302 switches in a grid from 1 to 35. Because we simulated the process of host-switching on
303 the complete primate phylogeny (367 species) and that HOME can only estimate host-
304 switches occurring between lineages present in the reconstructed phylogenetic tree
305 (composed of only 18 species), we expected HOME to infer fewer switches than
306 simulated (Table 1). As for ALE, we assessed the significance of the estimated scenario
307 of vertical transmission by performing 100 randomizations shuffling the associations
308 between host and OTU strains (*null model 2*). We considered that an OTU was
309 vertically transmitted if both the estimated substitution rate and the observed number
310 of host-switches were lower than 95% of the null expectations. Because HOME does
311 not tolerate multiple OTU strains per host tip at present, when simulations included
312 duplications, we randomly picked one single strain per host species. We ran HOME
313 only for alignments that had at least one segregating site.

314

315 We computed the statistical power as the percentage of OTUs simulated as
316 vertically transmitted (strictly vertically transmitted or vertically transmitted with
317 host-switches) that were correctly inferred as being vertically transmitted and the
318 type-I error rate as the percentage of OTUs simulated as independently evolving that
319 were incorrectly inferred as being vertically transmitted. We also measured the
320 computation time of the different approaches using a random subset of simulations.
321 For event-based approaches, we also evaluated the accuracy of parameter estimation.

322

323 **Empirical application:**

324

325 We downloaded the dataset from Amato *et al.* (2019) characterizing the gut
326 bacterial microbiota of 153 primates belonging to 18 species using the V4 region of the
327 16S rRNA gene available at <https://www.ebi.ac.uk/ena/data/view/PRJEB22679>. The
328 demultiplexed Illumina reads were processed using a pipeline based on VSEARCH
329 (Rognes, Flouri, Nichols, Quince, & Mahé, 2016) available at
330 <https://github.com/BPerezLamarque/Scripts/>. In short, after quality filtering, the reads
331 were clustered into OTUs using either Swarm clustering (Mahé, Rognes, Quince, de
332 Vargas, & Dunthorn, 2015) or traditional OTU clustering methods with 95% or 97%
333 sequence similarity thresholds using VSEARCH. We tested different OTU clustering
334 methods because we cannot know *a priori* which clustering method will delineate a

335 given OTU at the “right” level (*i.e.* not merging two biological units within the same
336 OTU, nor over-splitting one biological unit into two OTUs; Perez-Lamarque & Morlon,
337 2019). Chimeras were filtered out *de novo* and taxonomy was assigned to each OTU
338 using the Silva database (Quast et al., 2013). We kept only non-chimeric bacterial OTUs
339 represented by at least 5 reads in at least 2 samples. Finally, we assumed that if an OTU
340 had less than 5 reads in a sample, it was likely cross-contamination and set its
341 abundance to 0. For Swarm clustering, we obtained 6,373 OTUs representing a total of
342 4,019,271 reads, while clusterings at 97% and 95% gave 5,624 and 4,663 OTUs
343 respectively (corresponding to a total of 4,088,586 and 4,300,861 reads).

344

345 The ability to detect vertical transmission for a particular OTU depends on the
346 ability to detect this OTU across species in the first place, which can depend on a
347 number of factors during DNA extraction, PCR amplification, and sequencing. We
348 therefore evaluated whether we successfully detected most of the OTUs present within
349 samples and primate species by performing rarefaction analyses using the *vegan* R-
350 package (Oksanen et al., 2016).

351

352 We tested the support for vertical transmission only for “core OTUs”, taken to
353 be OTUs present in at least 10 out of the 18 primate species represented in the dataset.
354 First, we built a dataset with only one OTU strain per host species: for each OTU, we
355 merged all the primate samples from the same species together and built the alignment
356 by picking per host species the most abundant strain assigned to this OTU. We aligned
357 OTU strains using MAFFT (Katoh & Standley, 2013). We recorded the number of
358 segregating sites and unique strains in the resulting alignments and we applied
359 ParaFit, PACo, ALE, and HOME to detect vertically transmitted OTUs. Given that our
360 simulations highlighted a high type-I error rate for the correlative approaches and
361 ALE, and a low statistical power for HOME, when the number of segregating sites and
362 the number of hosts are low (see Results), we compared the distribution of these
363 characteristics in OTUs inferred to be vertically transmitted or not by the different
364 approaches. A comparatively low number of segregating sites and/or hosts in OTUs
365 inferred to be vertically transmitted by the correlative approaches and ALE would
366 suggest a lot of false positives. A comparatively high number of segregating sites
367 and/or hosts in OTUs inferred to be vertically transmitted by HOME would suggest
368 that some vertically transmitted OTUs might be missed (false negatives).

369

370 Next, we relaxed the hypothesis of a single OTU strain per host species, by
371 considering the possibility of multiple strains, resulting for instance, from intra-host
372 duplications: we picked up to 3 OTU strains per host species by selecting the 3 most

373 abundant ones when available. Given that HOME cannot tolerate multiple OTU
374 strains per host, we only ran ParaFit, PACo, and ALE.

375

376 Finally, for the OTUs that presented a significant cophylogenetic pattern
377 according to the different approaches, we tested whether this cophylogenetic pattern
378 could come from a geographic effect rather than from vertical transmission. Indeed, as
379 noted by Amato *et al.* (2019), a cophylogenetic pattern in primate microbiota could
380 arise because of the geographic split of the primates between the Old World (Africa
381 and Asia) and the New World (Americas). Heterogeneous environmental pools of
382 microbes in the Old and New Worlds combined with the fact that closely related
383 primate species tend to be present in the same area could generate cophylogenetic
384 patterns in the absence of vertical transmission. To test this, we randomized the
385 associations between primate species and OTU strains within the Old World and New
386 World respectively, and re-ran the analyses. If we still detect a significant
387 cophylogenetic pattern, we cannot reject the hypothesis that this pattern (at least
388 partially) comes from heterogeneous pools of microbes between the Old World and
389 the New World. Conversely, if we no longer detect a significant cophylogenetic
390 pattern, we can reject this hypothesis, therefore suggesting that the cophylogenetic
391 pattern is linked to vertical transmissions. An alternative (and faster) way for event-
392 based approaches to test this would be to use post-processing of the inferences to
393 assess whether the host-switches inferred by ALE and HOME tend to be more frequent
394 between host lineages present on the same continents (Perez-Lamarque *et al.*, 2022).
395 Here, for the sake of comparisons between global-fit and event-based approaches, we
396 evaluated the hypothesis of different geographic pools of microbes using
397 randomizations.

398 **Results:**

399

400 **Computational efficiency**

401

402 Global-fit approaches, especially ParaFit, were the fastest (Table 2). Their
403 computation time using 10,000 randomizations increased slightly with higher
404 simulated substitution rates (μ), but remained on average lower than one minute
405 (when measured on an Intel 2.8 GHz MacOSX laptop using only 1 CPU; Table 2;
406 Supplementary Fig. 2). In contrast, both event-based approaches were much slower,
407 even though we used only 100 randomizations to evaluate their significance. The
408 computation time of HOME increased with increasing μ ; from only a few hours when
409 the number of segregating sites was very low, to several hours or a few days when
410 there were many of them (Table 2). The computation time of ALE increased with
411 decreasing μ , linked to an increase of phylogenetic uncertainty in the trees of OTU
412 strains that slows down the reconciliation between these trees and the host phylogeny.
413 ALE sometimes took several days to run for a single OTU with $\mu=0.05$ (Table 2;
414 Supplementary Fig. 2). It also significantly increased in the presence of duplications.

415

416 To save time and energy, for each combination of simulated parameters, we ran
417 ALE and HOME on only 50 simulated alignments (against 100 for global-fit
418 approaches), except for $\mu=0.05$, where we used 100, given that many of the resulting
419 alignments contained no segregating sites. In addition, we did not run ALE when
420 $\mu=0.05$ and did not use HOME for alignments simulated with both $\mu>0.5$ and
421 duplications.

422

423

424 **Simulations without duplications or losses**

425

426 The alignments simulated without duplications or losses contained a mean
427 number of segregating sites larger than 20 and a mean number of strains larger than
428 15 (almost one OTU strain for each host species) when the simulated substitution rate
429 (μ) equaled 1.5. With $\mu=0.05$, they contained less than 5 segregating sites (with many
430 alignments presenting no segregating sites; Supplementary Fig. 1) and less than 5
431 strains.

432

433 Simulating up to 20 host-switches on the complete primate phylogeny had a
434 limited impact on the statistical performances of the different approaches (see
435 Supplementary Figs. 2-17). Therefore, we hereafter pooled all simulations of vertical

436 transmission (*i.e.* strict or with host-switches) when reporting estimations of statistical
437 power.

438

439 We found that global-fit approaches (ParaFit and PACo) have a high statistical
440 power ($\geq 98\%$) when $\mu \geq 0.5$ regardless of the null model used to assess statistical
441 significance (Figure 2). Their power decreases to $\sim 70\%$ when $\mu = 0.05$ (Supplementary
442 Figs. 3 & 4). However, they also have a rather elevated type-I error rate when $\mu = 0.05$
443 (type-I error rate $\sim 10\%$ for both ParaFit and PACo). With null model 1, PACo has a
444 type-I error rate $> 5\%$ even when μ is high (Supplementary Fig. 4).

445

446 ALE has a high power ($> 95\%$) and a low type-I error ($< 5\%$) when $\mu \geq 0.5$, using
447 either the criteria of Dorrell et al. (2021) or Groussin et al. (2017) for rejecting the null
448 hypothesis of independent evolution (Figure 2; Supplementary Figs. 5a and 6). In
449 simulations with strict vertical transmission, it correctly infers exclusively
450 codivergence events (and their approximate number, *i.e.* 17 on an 18 species tree,
451 Supplementary Fig. 5b). ALE also infers host-switches when simulated, although their
452 number is underestimated (Supplementary Fig. 5b). In simulations with independent
453 evolution, *i.e.* when there is no 'correct' reconciliation scenario, ALE estimates a lower
454 number of codivergence events and a much higher number of host-switches, as
455 expected (Supplementary Fig. 5b). However, with less segregating sites ($\mu = 0.1$), the
456 power of ALE is below 50%, the type-I error increases to 6%, and the inference of
457 reconciliation events is not accurate (Supplementary Fig. 5a&b and 6). Indeed, ALE
458 estimates many spurious losses and hosts-switches in simulations with strict vertical
459 transmission, and underestimates the number of host-switches in simulations with
460 host-switches (Supplementary Fig. 5b). The statistical power of ALE is even lower
461 (below 20% for $\mu = 0.1$, Supplementary Fig. 6) when following the criterium of Groussin
462 et al. (2017) than that of Dorrell et al. (2021); we thus kept the latter for rejecting the
463 null hypothesis of independent evolution when using ALE in the following analyses.

464

465 HOME has a high power ($> 94\%$) when $\mu \geq 0.5$ (Figure 2; Supplementary Fig. 7a),
466 but its statistical power decreases a lot with small μ values: with $\mu = 0.1$, the power of
467 HOME is below 40%, and with $\mu = 0.05$ below 25%. HOME has a low type-I error rate
468 ($< 5\%$) in all conditions, including when μ is low (Supplementary Fig. 7a). In terms of
469 inferred parameters, HOME correctly estimates the substitution rate. We cannot
470 directly test if the number of host-switches is well recovered, as HOME infers switches
471 on the provided tree (with 18 species) rather than on the complete tree, but we find
472 that HOME infers more host-switches when more are simulated (at least with
473 sufficient segregating sites, Supplementary Fig. 7b). In simulations with independent

474 evolution, *i.e.* when the evolution of the microbial DNA sequences on the host
475 phylogeny fits poorly, HOME estimates both high substitution rates and a high
476 number of host-switches, as expected (Supplementary Fig. 7b).

477

478 **Simulations with losses or/and duplications**

479

480 When simulating losses (or non-detection within hosts), the statistical power of
481 all the approaches decreases (Supplementary Figs. 8-10), especially for HOME (~10%
482 when $\mu=0.05$). For simulations with low μ values, the type-I error rate increases
483 strongly (>10%) for global-fit approaches and ALE, but not HOME (0% when $\mu=0.05$).
484 The type-I error rates of global-fit approaches decrease when using null model 2
485 instead of null model 1 (Supplementary Figs. 8).

486

487 Simulations with duplications generated alignments with a higher number of
488 segregating sites and strains (Supplementary Fig. 11). Under this scenario, we found
489 that the statistical power of global-fit approaches remains very high (>60% for all μ ;
490 Supplementary Fig. 12). The type-I error rate increases strongly under null model 1,
491 reaching 20% for PACo when $\mu=1.5$, but it can be reduced to 5% by using null model
492 2. ALE handles duplications very well, conserving a high power (>95%) and a low
493 type-I error rate (<5%; Supplementary Fig. 13). However, the computation time of the
494 approach increases substantially, which complicates the use of the method when the
495 number of segregating sites in the alignment is low. Finally, HOME, which cannot
496 consider multiple OTU strains per extant host, is not substantially affected by the
497 sampling at random of a single OTU strain per host: its power is intermediate and its
498 type-I error rate remains at 0% (Supplementary Fig. 14).

499

500 When simulating duplications and losses (or non-detection within hosts), we
501 observed similar trends with an overall decrease in the power of all the approaches,
502 an increase of the type-I error rate of ALE to 5%, and an increase of the type-I error
503 rate of PACo under null model 1 (but not null model 2; Figure 2; Supplementary Figs.
504 15-17). Increasing the number of randomizations to 100,000 in our significance test
505 does not fix this high type-I error, and more generally does not increase the
506 performances of PACo (Supplementary Fig. 18).

507

508

509 Empirical application

510

511 Rarefaction analyses on the gut microbiota of the 18 primate species revealed
512 that the sequencing depth used in each sample was sufficient to saturate per-sample
513 OTU richness, and that Shannon indices per species also reached a plateau when
514 increasing the number of samples (Supplementary Fig. 19). We found a total of 149
515 95% OTUs, 86 97% OTUs, and 47 Swarm OTUs that are “core OTUs” present in more
516 than 50% of the primate species. These core OTUs are on average detected in 12 host
517 species, and represent a minor fraction of the total number of reads in the primate gut
518 microbiota (28%, 14%, and 7%, respectively). The number of segregating sites and
519 strains in their alignments is similar to those of the OTUs simulated using substitution
520 rates ranging from $\mu=0.05$ to $\mu=0.5$ (Supplementary Figs. 1 & 20). The majority of these
521 core OTUs present a significant cophylogenetic pattern when using global-fit
522 approaches or ALE, corresponding to between 14% (based on 95% OTUs) and 2%
523 (based on Swarm OTUs) of the total number of reads of the primate gut microbiota
524 (Figure 3a). Conversely, HOME detected a significant cophylogenetic pattern in only
525 20% of the tested OTUs, corresponding to less than 7% of the total number of reads.
526 The different approaches agreed on a small set of OTUs (10% of the core 95% OTUs)
527 for which the cophylogenetic pattern is significant regardless of the approach used
528 (Figure 3b). As expected, in OTUs without a cophylogenetic pattern, ALE inferred a
529 lot of host-switches compared to codivergences (Supplementary Fig. 21), and HOME
530 inferred high substitution rates and many host-switches (Supplementary Fig. 22). In
531 OTUs with a significant cophylogenetic pattern, both methods inferred fewer, but a
532 still significant number (~5) of host-switches.

533

534 The much higher number of OTUs with a cophylogenetic pattern according to
535 global-fit approaches and ALE compared to HOME could be linked to the higher type-
536 I error rate of global-fit approaches and ALE, to the lower statistical power of HOME,
537 or both. When we compared the number of segregating sites and hosts of the OTUs
538 with or without a cophylogenetic pattern, we found that OTUs with a cophylogenetic
539 pattern in global-fit approaches and ALE have less nucleotide variation and are
540 present in a smaller number of hosts (Supplementary Fig. 19). The high type-I error
541 rate of these approaches under these conditions (Supplementary Figs. 2-10) suggests
542 that many of the OTUs for which they detected a cophylogenetic pattern are false
543 positives. Conversely, OTUs with a cophylogenetic pattern according to HOME have
544 more nucleotide variation and are present in a larger number of hosts. The gain of
545 power of HOME with increased information (Supplementary Figs. 2-10) suggests that
546 some vertically transmitted OTUs with little nucleotide variation or present in a few

547 hosts were missed by the method. Hence, both the high type-I error rate of global-fit
548 approaches and ALE and the low statistical power of HOME probably contribute to
549 the contrasting results they provide.

550

551 When selecting several OTU strains per host species and applying global-fit
552 approaches and ALE, more than 75% of the tested OTUs presented a significant
553 cophylogenetic pattern (Supplementary Fig. 23). However, the type-I error rate of
554 these approaches is higher when there are multiple strains per host species (especially
555 PACo; Supplementary Figs. 12-17), suggesting that many of these OTUs are false
556 positives.

557

558 Our test of geographically-driven cophylogenetic patterns between the Old
559 World and the New World revealed that, at least for these data, HOME is more likely
560 than the other approaches to identify OTUs that are truly vertically transmitted (Figure
561 4). Indeed, the majority of OTUs with a significant cophylogenetic pattern inferred
562 with ParaFit, PACo, and ALE still had a significant cophylogenetic pattern when
563 randomizing the associations between primate species and OTU strains within the Old
564 and New Worlds. Conversely, the majority of OTUs with a significant cophylogenetic
565 pattern inferred with HOME no longer had this cophylogenetic pattern when
566 randomizing the associations between primate species and OTU strains based on
567 geography, as expected if the pattern arises from vertical transmission rather than
568 geographically structured pools of microbes. 24 out of the 149 'core' 95% OTUs (*i.e.*
569 16% of them) presented a cophylogenetic pattern that did not arise from geographic
570 structure according to HOME, corresponding to at most 5% of the total number of
571 reads of the primate gut microbiota (Figure 4). We considered that these OTUs are
572 likely to be vertically transmitted (but see Discussion). These vertically transmitted
573 bacteria belonged mostly to the class Clostridia (phylum Firmicutes), especially the
574 orders Lachnospirales and Oscillospirales, and to a lesser extent to the class Bacilli
575 (phylum Firmicutes).

576 **Discussion:**

577

578 In this study, we used simulations to compare the statistical performances of
579 different global-fit and event-based approaches to detect vertically transmitted OTUs
580 in microbiota characterized by DNA metabarcoding. We found that the different
581 approaches are rather complementary (Table 2). Their application to primate gut
582 microbiota identifies vertically transmitted bacterial OTUs that represent a small
583 fraction (~5%) of the total number of reads.

584

585 **Pros and cons of different quantitative approaches to detect vertical transmission:**

586

587 The main advantage of global-fit methods is their computational efficiency.
588 Depending on the size of the dataset in hand, there might be no other choice than to
589 use these methods instead of event-based approaches. Global-fit methods generally
590 have high statistical power. Also, they are robust to the presence of up to an
591 intermediate number host-switches even though, unlike event-based approaches, they
592 do not explicitly model these events. However, they also have an elevated type-I error
593 rate when there are only a few segregating sites in the alignment. Although global-fit
594 approaches typically use a randomization technique that independently randomizes
595 which host species are associated with each OTU strain ("null model 1"), we found
596 that shuffling the host species names instead ("null model 2"), as done in event-based
597 approaches, reduces their type-I error. Null model 2 conserves the structure of the
598 interactions, while null model 1 conserves only the number of host species associated
599 with each OTU strain, which is less conservative. We therefore recommend using null
600 model 2 in this context. Given that PACo tends to often have a higher type-I error than
601 ParaFit and takes more time to run, we also recommend using ParaFit over PACo to
602 detect vertically transmitted OTUs. Even when using ParaFit with null model 2,
603 global-fit approaches have a higher type-I error rate than event-based ones. Although
604 this would require further testing with simulations, our empirical analyses suggest
605 that global-fit approaches have the highest difficulty to distinguish a geographic
606 structure in the data from the signal of vertical transmission. These results suggest that
607 event-based approaches should be preferred over global-fit ones when possible.

608

609 ALE outperforms all the other approaches on simulated data when OTUs have
610 accumulated enough divergence, *i.e.* >10 segregating sites and/or >8 unique strains in
611 the context of our simulations (Table 2). It not only has high power and a low type-I
612 error rate, but it also accurately fits reconciliation events (host-switches, duplications,
613 and losses) between the hosts and the trees of OTU strains. To evaluate the significance

614 of the reconciled scenarios, we recommend separately comparing the number of
615 codivergences and host-switches against null expectations (as in Dorrell et al. 2021),
616 rather than looking at the differences between the number of codivergences and host-
617 switches (as in Groussin *et al.*, 2017), as the latter strategy decreases the statistical
618 power of the approach. ALE does not perform as well under situations with a low
619 number of segregating sites. In this case, there is a lot of uncertainty in the
620 reconstructed trees of OTU strains, and ALE is very slow to run. In addition, in this
621 situation ALE has a higher type-I error rate when the OTU is not present in all host
622 species (*i.e.* when there are losses), which is frequently the case in empirical data. We
623 therefore do not recommend using ALE when the amount of variation in the OTU
624 strains is too low. Also, while ALE has a much higher power than HOME and a low
625 type-I error rate on simulated data with enough segregating sites, our results on
626 empirical data suggest that ALE is in fact not conservative enough in its inference of
627 vertical transmission. In particular, our empirical results suggest that ALE does not
628 easily distinguish a geographic structure in the data from vertical transmission.

629

630 In contrast to the other approaches, HOME keeps a low type-I error rate, at least
631 under all the situations we tested. The major drawback of HOME is that it has limited
632 power. Another drawback is not handling multiple OTU strains per host species. In
633 the presence of multiple strains, a user of HOME can randomly sample a single strain
634 per host. However, as we showed in our simulations with within-host duplications,
635 this contributes to further decreasing the statistical power of HOME. Therefore,
636 HOME should be used only when within-host duplications are infrequent. On the
637 positive side, in addition to the low type-I error rate, our empirical results suggest that
638 HOME can often distinguish a geographic structure in the data from vertical
639 transmission. This should ideally be tested further with simulations including
640 heterogeneous pools of environmental microbes and phylogenetic signal in the host
641 geographic distributions.

642

643 The distinct statistical performances of the different approaches can be
644 explained by their constructions. Global-fit approaches do not model underlying
645 processes, and therefore do not perform as well as event-based approaches. HOME
646 seems to be less likely than global-fit approaches or ALE to infer vertical transmission
647 for OTUs that present a strong geographical signal, which is likely due to the fact that
648 HOME directly models DNA substitutions on the host phylogeny. For example, if the
649 pools of OTU strains differ between the New and Old Worlds, they are unlikely to be
650 particularly well modeled by a substitution process on the host tree, and the model
651 therefore rejects the hypothesis of vertical transmission. Other processes than vertical

652 transmission and geographic structure can generate a cophylogenetic pattern between
653 host and trees of OTU strains (de Vienne et al., 2013), and statistical methods that are
654 based on models that can represent these processes are more likely to perform better
655 than those that do not.

656

657 We limited our analyses to the comparisons of four computational approaches
658 that have previously been used for detecting vertical transmission in host-associated
659 metabarcoding datasets. One of them (ALE) was originally developed for species-gene
660 reconciliations purposes. Other approaches have been developed in this context, and
661 could potentially also be useful for detecting vertical transmission (e.g. Bansal, Kellis,
662 Kordi, & Kundu, 2018; Jacox, Chauve, Szölloši, Ponty, & Scornavacca, 2016; Morel,
663 Kozlov, Stamatakis, & Szöllősi, 2020), which could be explored in future simulation
664 and empirical works. Meanwhile, we suggest simultaneously combining several
665 approaches: ParaFit (and ALE when there are enough segregating sites) may be used
666 to identify a larger set of potentially vertically transmitted OTUs, some of which might
667 be false positives, while HOME may be used to identify a conservative set of vertically
668 transmitted OTUs. The right number of vertically transmitted OTUs is likely included
669 between both estimates.

670

671 In other non-bacterial systems, such as host-macroparasite systems, genetic
672 data and species delineation for the parasites are generally of better quality than those
673 obtained with metabarcoding data. We can use our comparison of statistical
674 performances under simulations with high substitution to guide the choice of method
675 to use in this case. For such systems, we recommend using ALE (with the Dorrell et al.
676 (2021) criteria) when computationally feasible, and ParaFit (with null model 2)
677 otherwise. When a cophylogenetic pattern is detected, we recommend carefully
678 checking that this pattern is not linked to geographic structure in the data. Other event-
679 based approaches that do not consider phylogenetic uncertainty and rely on maximum
680 parsimony, *e.g.* eMPress (Santichaivekin et al., 2021), are also likely to be valuable
681 tools for detecting vertical transmission in such systems.

682

683 **Vertical transmission in the primate gut microbiota:**

684

685 We observed quantitative differences in the number of bacterial OTUs with a
686 significant cophylogenetic pattern according to the different OTU clustering we
687 performed. In particular, we detected >2 times fewer 'core' OTUs when using the
688 Swarm clustering, resulting in >2 times fewer OTUs with a cophylogenetic pattern,
689 maybe because this clustering method over-splits vertically transmitted bacteria that

690 have accumulated too many divergences (Perez-Lamarque & Morlon, 2019). Using
691 approaches that can handle multiple OTU strains per host species, we found many
692 OTUs with a cophylogenetic pattern. These are likely false positives, given the high
693 type-I error rate of these approaches in such conditions. These results suggest that
694 when it is not clear whether multiple OTU strains correspond to real biological units
695 and not PCR or sequencing error artifacts, it is preferable to simply pick the most
696 abundant strain per host species and ignore duplication events.

697

698 Ideally, to assess whether cophylogenetic patterns were generated by vertical
699 transmission, one also has to test whether the divergence times for the hosts match
700 those of the OTU strains (de Vienne et al., 2013). We cannot robustly reconstruct the
701 trees of OTU strains here, but we can examine the number of segregating sites, which
702 range between 2 and 15 (within a single OTU) across bacterial OTUs from the primate
703 gut. Given that the 16S rRNA gene diverges on average by 1% every 50 million years
704 (Myr) (Ochman, Elwyn, & Moran, 1999), and that the primates are >65 Myr old, a
705 metabarcoding marker with less than 10 segregating sites suggests divergence times
706 for the OTU strains that match those of the hosts. Most of our alignments meet this
707 criterium. When the number of segregating sites exceeds 10 (especially for 95% OTUs),
708 alignments might either correspond to conglomerates of several vertically transmitted
709 OTUs (Perez-Lamarque & Morlon, 2019) or to fast-evolving bacteria, like vertically
710 transmitted bacteria with small population sizes (Moran, Munson, Baumann, &
711 Ishikawa, 1993).

712

713 When removing OTUs whose cophylogenetic pattern arose from a phylogenetic
714 signal in host geographic distribution, we estimated that less than 15% of the 'core'
715 OTUs present in the gut microbiota of more than 50% of the primate species are
716 vertically transmitted. These OTUs only represent a small fraction (~5%) of the total
717 number of bacterial reads. Accounting for the sometimes low statistical power of the
718 approaches we used (<50% in some conditions), we may conclude that at most 30% of
719 the 'core' OTUs in the bacterial gut microbiota of primates are vertically transmitted.
720 Given that mammal gut microbiota can be composed of a large proportion of transient
721 food-derived and/or environment-specific microbes that are unlikely to be faithfully
722 vertically transmitted over more than 50 Myr (Amato et al., 2019; Nishida & Ochman,
723 2019), this estimate seems more realistic than larger ones. Among the bacteria inferred
724 to be vertically transmitted, we found a large proportion in the order Clostridia
725 (phylum Firmicutes), as found in previous analyses (Gaulke et al., 2018; Groussin et
726 al., 2017; Perez-Lamarque & Morlon, 2019).

727

728

729 **Conclusion:**

730

731 Looking at vertically transmitted OTUs using metabarcoding datasets is
732 challenging because of the low amount of information contained in metabarcoding
733 marker genes. The different approaches that can be used for this purpose have
734 complementary advantages and weaknesses. We recommend combining HOME,
735 which has very infrequent false positives but limited power, with ALE (when there is
736 enough variation in the alignments) or ParaFit, which have a higher power but many
737 false positives. The 'right' number of vertically transmitted OTUs is likely between the
738 estimates obtained with these approaches. We also recommend performing further
739 checks, such as randomizing the host-bacteria associations within the main geographic
740 areas of host distribution, in order to test whether the detected cophylogenetic patterns
741 may have been generated by other processes than vertical transmissions. Applied to
742 the gut microbiota of primates, we confirm that gut bacteria can be vertically
743 transmitted, although most of the gut microbiota is not. Future work focusing on the
744 specificities of these vertically transmitted bacteria would provide a better
745 understanding of the mechanisms favoring vertical transmission for some particular
746 bacterial lineages.

747

748

749 **Data Accessibility and Benefit-Sharing Section:**

750

751 Data Accessibility Statement: ParaFit, PACo, and HOME are available as R functions.
752 A tutorial on how to use HOME is available at
753 <https://github.com/BPerezLamarque/HOME/>. Amended functions of ParaFit and
754 PACo (from the R-packages ape (Paradis et al., 2004) and paco (Hutchinson et al.,
755 2017)) are available at: [https://github.com/BPerezLamarque/
756 Scripts/tree/master/Comparing_methods_vertical_transmission/](https://github.com/BPerezLamarque/Scripts/tree/master/Comparing_methods_vertical_transmission/). ALE requires the
757 installation of PhyloBayes and the software ALE (<https://github.com/ssolo/ALE/>) and
758 is executable on a terminal; a tutorial is available at
759 <https://github.com/ssolo/ALE/#using-ale>.

760 Both our scripts and simulations (DNA alignments of the OTUs) are publicly
761 accessible through the Open Science Framework (osf) portal: osf.io/2rw36/. Raw data
762 for the empirical analyses (from Amato et al. (2019)) are available at:

763 <https://www.ebi.ac.uk/ena/data/view/PRJEB22679>.

764

765 Benefits Generated: Benefits from this research accrue from the sharing of our data and
766 results on public databases as described above.

767

768

769 **Author contributions:**

770

771 BPL and HM designed the study. BPL performed the analyses. BPL and HM wrote the
772 manuscript.

773

774

775 **Acknowledgments:**

776

777 The authors acknowledge members of the BioDiv team at IBENS, V. Daubin, and B.
778 Boussau for helpful discussions, as well as the Editor and three anonymous referees
779 for their constructive comments. This work was supported by a doctoral fellowship
780 from the École Normale Supérieure de Paris attributed to BPL. HM acknowledges
781 support from the European Research Council (grant CoG-PANDA).

782 **References:**

783

- 784 Amato, K. R., G. Sanders, J., Song, S. J., Nute, M., Metcalf, J. L., Thompson, L. R., ...
785 Stumpf, R. M. (2019). Evolutionary trends in host physiology outweigh dietary
786 niche in structuring primate gut microbiomes. *The ISME Journal*, *13*(3), 576–587.
787 doi:10.1038/s41396-018-0175-0
- 788 Balbuena, J. A., Míguez-Lozano, R., & Blasco-Costa, I. (2013). PACo: A novel
789 procrustes application to cophylogenetic analysis. *PLoS ONE*, *8*(4), e61048.
790 doi:10.1371/journal.pone.0061048
- 791 Bansal, M. S., Kellis, M., Kordi, M., & Kundu, S. (2018). RANGER-DTL 2.0: Rigorous
792 reconstruction of gene-family evolution by duplication, transfer and loss.
793 *Bioinformatics*, *34*(18), 3214–3216. doi:10.1093/bioinformatics/bty314
- 794 Blasco-Costa, I., Hayward, A., Poulin, R., & Balbuena, J. A. (2021). Next-generation
795 cophylogeny: unravelling eco-evolutionary processes. *Trends in Ecology and*
796 *Evolution*, *36*(10), 907–918. doi:10.1016/j.tree.2021.06.006
- 797 De Vienne, D. M., Giraud, T., & Shykoff, J. A. (2007). When can host shifts produce
798 congruent host and parasite phylogenies? A simulation approach. *Journal of*
799 *Evolutionary Biology*, *20*(4), 1428–1438. doi:10.1111/j.1420-9101.2007.01340.x
- 800 de Vienne, D. M., Refrégier, G., López-Villavicencio, M., Tellier, A., Hood, M. E., &
801 Giraud, T. (2013). Cospeciation vs host-shift speciation: Methods for testing,
802 evidence from natural associations and relation to coevolution. *New Phytologist*,
803 *198*(2), 347–385. doi:10.1111/nph.12150
- 804 Dismukes, W., Braga, M. P., Hembry, D. H., Heath, T. A., & Landis, M. J. (2022).
805 Cophylogenetic methods to untangle the evolutionary history of ecological
806 interactions. *Annual Review of Ecology, Evolution, and Systematics*, *53*(1), 1–24.
807 doi:10.1146/annurev-ecolsys-102320-112823
- 808 Dorrell, R. G., Villain, A., Perez-Lamarque, B., Audren de Kerdrel, G., McCallum, G.,
809 Watson, A. K., ... Blanc, G. (2021). Phylogenomic fingerprinting of tempo and
810 functions of horizontal gene transfer within ochrophytes. *Proceedings of the*
811 *National Academy of Sciences*, *118*(4), e2009974118. doi:10.1073/pnas.2009974118
- 812 Dos Reis, M., Gunnell, G. F., Barba-Montoya, J., Wilkins, A., Yang, Z., & Yoder, A. D.
813 (2018). Using phylogenomic data to explore the effects of relaxed clocks and
814 calibration strategies on divergence time estimation: Primates as a test case.
815 *Systematic Biology*, *67*(4), 594–615. doi:10.1093/sysbio/syy001
- 816 Gaulke, C. A., Arnold, H. K., Humphreys, I. R., Kembel, S. W., O'Dwyer, J. P., &
817 Sharpton, T. J. (2018). Ecophylogenetics clarifies the evolutionary association
818 between mammals and their gut microbiota. *MBio*, *9*(5), 1–14.
819 doi:10.1128/mBio.01348-18
- 820 Groussin, M., Mazel, F., Sanders, J. G., Smillie, C. S., Lavergne, S., Thuiller, W., &
821 Alm, E. J. (2017). Unraveling the processes shaping mammalian gut microbiomes
822 over evolutionary time. *Nature Communications*, *8*(1), 14319.
823 doi:10.1038/ncomms14319
- 824 Hacquard, S., Garrido-Oter, R., González, A., Spaepen, S., Ackermann, G., Lebeis, S.,

- 825 ... Schulze-Lefert, P. (2015). Microbiota and host nutrition across plant and
826 animal kingdoms. *Cell Host and Microbe*, 17(5), 603–616.
827 doi:10.1016/j.chom.2015.04.009
- 828 Hayward, A., Poulin, R., & Nakagawa, S. (2021). A broadscale analysis of host-
829 symbiont cophylogeny reveals the drivers of phylogenetic congruence. *Ecology*
830 *Letters*, 24(8), 1681–1696. doi:10.1111/ele.13757
- 831 Hommola, K., Smith, J. E., Qiu, Y., & Gilks, W. R. (2009). A permutation test of host-
832 parasite cospeciation. *Molecular Biology and Evolution*, 26(7), 1457–1468.
833 doi:10.1093/molbev/msp062
- 834 Hutchinson, M. C., Cagua, E. F., Balbuena, J. A., Stouffer, D. B., & Poisot, T. (2017).
835 paco: implementing Procrustean Approach to Cophylogeny in R. *Methods in*
836 *Ecology and Evolution*, 8(8), 932–940. doi:10.1111/2041-210X.12736
- 837 Jacox, E., Chauve, C., Szöllösi, G. J., Ponty, Y., & Scornavacca, C. (2016). EcceTERA:
838 Comprehensive gene tree-species tree reconciliation using parsimony.
839 *Bioinformatics*, 32(13), 2056–2058. doi:10.1093/bioinformatics/btw105
- 840 Katoh, K., & Standley, D. M. (2013). MAFFT Multiple sequence alignment software
841 version 7: Improvements in performance and usability. *Molecular Biology and*
842 *Evolution*, 30(4), 772–780. doi:10.1093/molbev/mst010
- 843 Kimura, M. (1980). A simple method for estimating evolutionary rates of base
844 substitutions through comparative studies of nucleotide sequences. *Journal of*
845 *Molecular Evolution*, 16(2), 111–120. doi:10.1007/BF01731581
- 846 Lartillot, N., & Philippe, H. (2004). A Bayesian mixture model for across-site
847 heterogeneities in the amino-acid replacement process. *Molecular Biology and*
848 *Evolution*, 21(6), 1095–1109. doi:10.1093/molbev/msh112
- 849 Legendre, P., Desdevises, Y., & Bazin, E. (2002). A statistical test for host-parasite
850 coevolution. *Systematic Biology*, 51(2), 217–234. doi:10.1080/10635150252899734
- 851 Mahé, F., Rognes, T., Quince, C., de Vargas, C., & Dunthorn, M. (2015). Swarmv2:
852 Highly-scalable and high-resolution amplicon clustering. *PeerJ*, 2015(12), 1–12.
853 doi:10.7717/peerj.1420
- 854 McFall-Ngai, M., Hadfield, M. G., Bosch, T. C. G., Carey, H. V., Domazet-Lošo, T.,
855 Douglas, A. E., ... Wernegreen, J. J. (2013). Animals in a bacterial world, a new
856 imperative for the life sciences. *Proceedings of the National Academy of Sciences*,
857 110(9), 3229–3236. doi:10.1073/pnas.1218525110
- 858 Moeller, A. H., Caro-Quintero, A., Mjungu, D., Georgiev, A. V, Lonsdorf, E. V,
859 Muller, M. N., ... Ochman, H. (2016). Cospeciation of gut microbiota with
860 hominids. *Science*, 353(6297), 380–382. doi:10.1126/science.aaf3951
- 861 Moran, N. A., Munson, M. A., Baumann, P., & Ishikawa, H. (1993). A molecular clock
862 in endosymbiotic bacteria is calibrated using the insect hosts. *Proceedings of the*
863 *Royal Society of London. Series B: Biological Sciences*, 253(1337), 167–171.
864 doi:10.1098/rspb.1993.0098
- 865 Moran, N. A., Ochman, H., & Hammer, T. J. (2019, November 2). Evolutionary and
866 ecological consequences of gut microbial communities. *Annual Review of Ecology,*
867 *Evolution, and Systematics*. Annual Reviews. doi:10.1146/annurev-ecolsys-110617-

- 868 062453
- 869 Morel, B., Kozlov, A. M., Stamatakis, A., & Szöllősi, G. J. (2020). GeneRax: A tool for
870 species-tree-aware maximum likelihood-based gene family tree inference under
871 gene duplication, transfer, and loss. *Molecular Biology and Evolution*, 37(9), 2763–
872 2774. doi:10.1093/molbev/msaa141
- 873 Nishida, A. H., & Ochman, H. (2019). A great-ape view of the gut microbiome. *Nature*
874 *Reviews Genetics*, 20(4), 195–206. doi:10.1038/s41576-018-0085-z
- 875 Ochman, H., Elwyn, S., & Moran, N. A. (1999). Calibrating bacterial evolution.
876 *Proceedings of the National Academy of Sciences*, 96(22), 12638–12643.
877 doi:10.1073/pnas.96.22.12638
- 878 Ochman, H., Worobey, M., Kuo, C. H., Ndjango, J. B. N., Peeters, M., Hahn, B. H., &
879 Hugenholtz, P. (2010). Evolutionary relationships of wild hominids
880 recapitulated by gut microbial communities. *PLoS Biology*, 8(11), 3–10.
881 doi:10.1371/journal.pbio.1000546
- 882 Oksanen, J., Kindt, R., Pierre, L., O'Hara, B., Simpson, G. L., Solymos, P., ... Wagner,
883 H. (2016). vegan: Community Ecology Package, R package version 2.4-0. *R*
884 *Package Version 2.2-1*.
- 885 Page, R. D. M. (1994). Parallel phylogenies: Reconstructing the history of host-
886 parasite assemblages. *Cladistics*, 10(2), 155–173. doi:10.1111/j.1096-
887 0031.1994.tb00170.x
- 888 Paradis, E., Claude, J., & Strimmer, K. (2004). APE: Analyses of phylogenetics and
889 evolution in R language. *Bioinformatics*, 20(2), 289–290.
890 doi:10.1093/bioinformatics/btg412
- 891 Perez-Lamarque, B., Krehenwinkel, H., Gillespie, R. G., & Morlon, H. (2022). Limited
892 evidence for microbial transmission in the phyllosymbiosis between Hawaiian
893 spiders and their microbiota. *MSystems*, 7(1). doi:10.1128/msystems.01104-21
- 894 Perez-Lamarque, B., & Morlon, H. (2019). Characterizing symbiont inheritance
895 during host–microbiota evolution: Application to the great apes gut microbiota.
896 *Molecular Ecology Resources*, 19(6), 1659–1671. doi:10.1111/1755-0998.13063
- 897 Quast, C., Pruesse, E., Yilmaz, P., Gerken, J., Schweer, T., Yarza, P., ... Glöckner, F. O.
898 (2013). The SILVA ribosomal RNA gene database project: Improved data
899 processing and web-based tools. *Nucleic Acids Research*, 41(D1), D590–D596.
900 doi:10.1093/nar/gks1219
- 901 R Core Team. (2022). R: A language and environment for statistical computing.
902 Vienna, Austria: R Foundation for Statistical Computing.
- 903 Rognes, T., Flouri, T., Nichols, B., Quince, C., & Mahé, F. (2016). VSEARCH: A
904 versatile open source tool for metagenomics. *PeerJ*, 2016(10), e2584.
905 doi:10.7717/peerj.2584
- 906 Sanders, J. G., Powell, S., Kronauer, D. J. C., Vasconcelos, H. L., Frederickson, M. E.,
907 & Pierce, N. E. (2014). Stability and phylogenetic correlation in gut microbiota:
908 lessons from ants and apes. *Molecular Ecology*, 23(6), 1268–1283.
909 doi:10.1111/mec.12611
- 910 Santichaivekin, S., Yang, Q., Liu, J., Mawhorter, R., Jiang, J., Wesley, T., ... Libeskind-

- 911 Hadas, R. (2021). EMPress: A systematic cophylogeny reconciliation tool.
912 *Bioinformatics*, 37(16), 2481–2482. doi:10.1093/bioinformatics/btaa978
- 913 Selosse, M. A., Baudoin, E., & Vandenkoornhuyse, P. (2004). Symbiotic
914 microorganisms, a key for ecological success and protection of plants. *Comptes*
915 *Rendus - Biologies*, 327(7), 639–648. doi:10.1016/j.crv.2003.12.008
- 916 Szöllősi, G. J., Rosikiewicz, W., Boussau, B., Tannier, E., Daubin, V., Szölloosi, G. J., ...
917 Daubin, V. (2013). Efficient exploration of the space of reconciled gene trees.
918 *Systematic Biology*, 62(6), 901–912. doi:10.1093/sysbio/syt054
- 919 Szöllősi, G. J., Tannier, E., Lartillot, N., Daubin, V., Szölloosi, G. J., Tannier, E., ...
920 Daubin, V. (2013). Lateral gene transfer from the dead. *Systematic Biology*, 62(3),
921 386–397. doi:10.1093/sysbio/syt003
- 922 Youngblut, N. D., Reischer, G. H., Walters, W., Schuster, N., Walzer, C., Stalder, G.,
923 ... Farnleitner, A. H. (2019). Host diet and evolutionary history explain different
924 aspects of gut microbiome diversity among vertebrate clades. *Nature*
925 *Communications*, 10(1), 1–15. doi:10.1038/s41467-019-10191-3
- 926
- 927

928 **Tables**

929

930

931 **Table 1: Main characteristics of the different cophylogenetic methods that can be**
 932 **used for detecting vertical transmission in host-associated microbiota.** ParaFit,
 933 PACo, and ALE were developed to study a broader array of host-symbiont
 934 associations. HOME was specifically designed to study host-microbiota associations
 935 from short (meta)barcoding data.

936

937

Method	ParaFit	PACo	ALE	HOME
Main feature	Global-fit approach: Measures the overall congruence between the host phylogeny and the microbial genetic distances using the fourth-corner statistic.	Global-fit approach: Measures the overall congruence between the host phylogeny and the microbial genetic distances using Procrustes superimposition.	Event-based approach: Models events of codivergence, host-switch, loss, and duplication to reconcile the host and microbial phylogenetic trees (reconstructed beforehand).	Event-based approach: Models the microbial DNA evolution on the host phylogenetic tree, while fitting potential host-switches.
Major assumptions	Identical OTU strains in different host species are considered as interchangeable.	Identical OTU strains in different host species are considered as interchangeable.	Assumes that most host lineages are not sampled or extinct; A host-switch always involves an unsampled lineage as an intermediate. Branch lengths are not considered (only the topologies and the relative order of nodes of the host tree are considered).	Models DNA evolution on the host phylogenetic tree, allowing for host-switches. OTU duplications and losses are not considered. Does not consider under-sampling or extinction of the host lineages.
Inputs	Pairwise (phylo)genetic distances for the hosts and their associated microbes	Pairwise (phylo)genetic distances for the hosts and their associated microbes	A rooted host phylogenetic tree and a posterior distribution of microbial phylogenetic trees (with at least one microbe per host species)	A time-calibrated host phylogenetic tree and a DNA alignment constituted of one microbial DNA strain per host species (at most)
Randomization strategy	Null model 1: Independent permutation of the host species associated with each microbial strain Null model 2: Permutation of the host species name in the host phylogenetic tree	Null model 1: Independent permutation of the host species associated with each microbial strain Null model 2: Permutation of the host species name in the host phylogenetic tree	Null model 2: Permutation of the host species name in the host phylogenetic tree	Null model 2: Permutation of the host species name in the host phylogenetic tree

938 **Table 2: Summary of the statistical performances of the different methods for**
939 **detecting vertical transmission in host-associated microbiota:**

940 For each method, we summarize its running time and its statistical performances
941 evaluated using simulations. The running time and statistical performances
942 correspond to the simulations without duplications or losses, with different
943 substitution rates for the microbial OTUs: $\mu=1.5$, $\mu=0.5$, and $\mu=0.05$. Global-fit
944 approaches were run with 10,000 randomizations, while we only used 100
945 randomizations for event-based ones. Computation times (mean \pm s.d.) were
946 measured on an Intel 2.8 GHz MacOSX laptop using only 1 CPU; for ALE, they
947 included the time to reconstruct the trees of OTU strains (e.g. using PhyloBayes),
948 which is longer when the substitution rate is high. The inference of HOME was
949 designed to run in parallel and is thus faster on multi-core processors. Details on the
950 statistical performances of the different approaches can be found in the supplements.
951

952

953

954

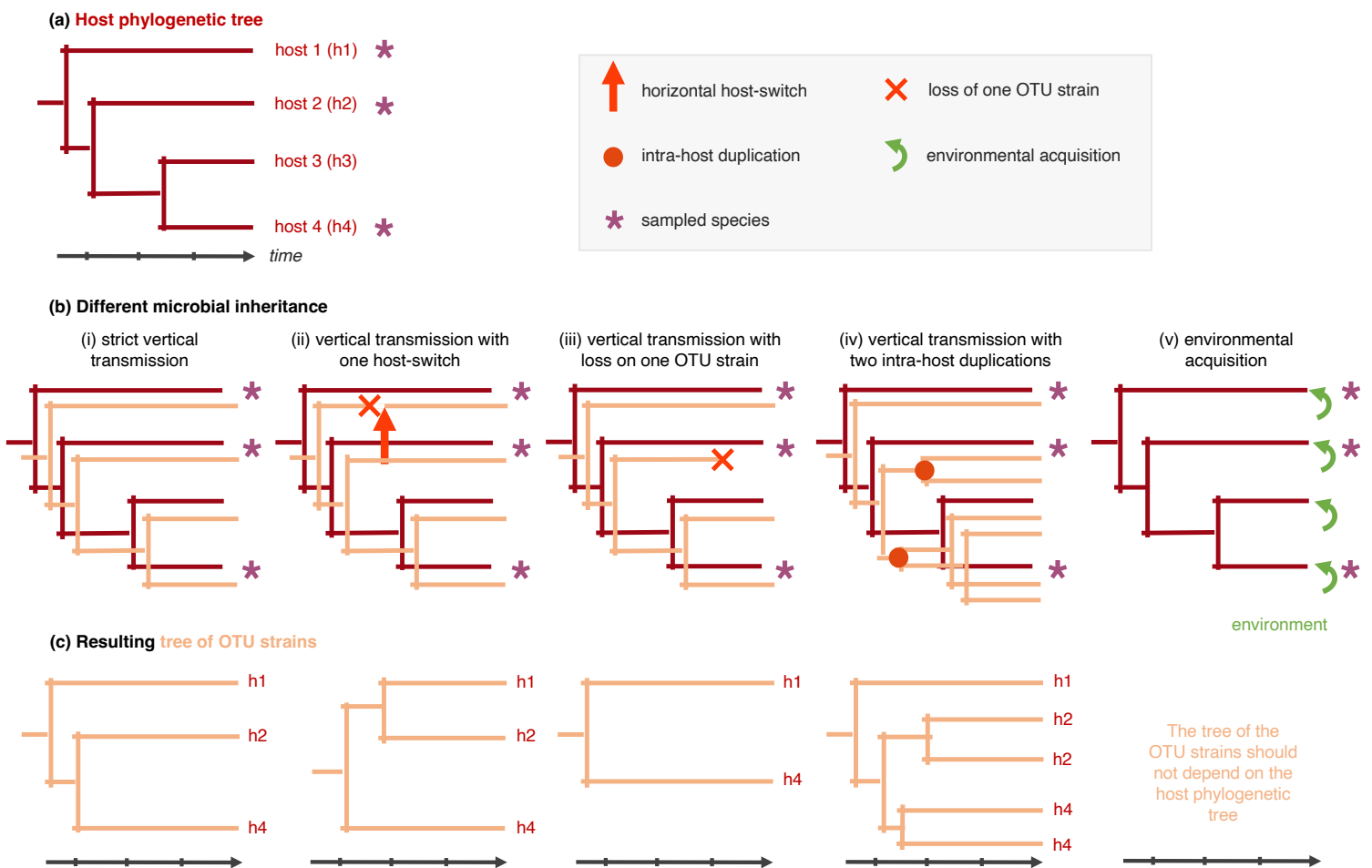
Method	ParaFit (null model 1)	ParaFit (null model 2)	PACo (null model 1)	PACo (null model 2)	ALE	HOME
Running time when $\mu = 1.5$	1.8 sec \pm 1		53.8 sec \pm 2.2		1.7 h \pm 0.8	26.8 h \pm 15.3
Running time when $\mu = 0.5$	1.5 sec \pm 0.8		49.1 sec \pm 1.9		5.7 h \pm 5.6	17.8 h \pm 11.7
Running time when $\mu = 0.05$	1.3 sec \pm 0.4		45.3 sec \pm 2.3		23.9 h \pm 8	2.2 h \pm 2.8
Performances when $\mu = 1.5$	Power: 100% Type-I error: 2%	Power: 100% Type-I error: 2%	Power: 100% Type-I error: 8%	Power: 100% Type-I error: 2%	Power: 100% Type-I error: 2%	Power: 100% Type-I error: 4%
Performances when $\mu = 0.5$	Power: 98% Type-I error: 1%	Power: 98% Type-I error: 1%	Power: 99% Type-I error: 3%	Power: 98% Type-I error: 2%	Power: 97% Type-I error: 2%	Power: 94% Type-I error: 4%
Performances when $\mu = 0.05$	Power: 73% Type-I error: 10%	Power: 71% Type-I error: 10%	Power: 68% Type-I error: 8%	Power: 72% Type-I error: 10%	Too slow to be run	Power: 23% Type-I error: 0%
Advantages	Very fast; High statistical power		Very fast; High statistical power		Fast when μ is high; Good statistical performances and estimation of many events of host- microbe evolution	Fast when μ is low; Low type-I error; Estimation of the host-switch dynamic;
Disadvantages	Does not model the processes of host- microbe evolution; High type-I error rate, especially when μ is low.		Does not model the processes of host- microbe evolution; High type-I error rate, especially when μ is low.		Slow when μ is low; Branch lengths are not considered; Does not model the timing of DNA evolution.	Slow when μ is high; Low power when μ is low; Cannot consider more than 1 microbial strain per host species

955 **Figures:**

956

957 **Figure 1: Different modes of inheritance of a given host-associated operational**
 958 **taxonomic unit (OTU) and their consequences on the microbial tree (tree of OTU**
 959 **strains).**

960 On a phylogenetic tree of 4 host species (a), we represent the different modes of
 961 inheritance for a given OTU (b) and the resulting tree of OTU strains (c). Each host is
 962 at least colonized by one strain of this given OTU (except in the case of OTU loss in
 963 (iii)). We also represent a sampling process where the microbiota of only some extant
 964 host species (marked by “*”) is characterized. Extreme scenarios correspond to strict
 965 vertical transmission (i; perfect cophylogenetic pattern) or environmental acquisition
 966 (v; no cophylogenetic pattern expected). In more intermediate scenarios, the perfect
 967 congruence between the host phylogeny and the tree of OTU strains, a characteristic
 968 of vertical transmission, is dampened by events of horizontal transmissions (ii; the
 969 horizontal host-switch from one donor host to a receiver host with replacement of the
 970 OTU strain), microbial loss (iii), or intra-host duplication (iv).

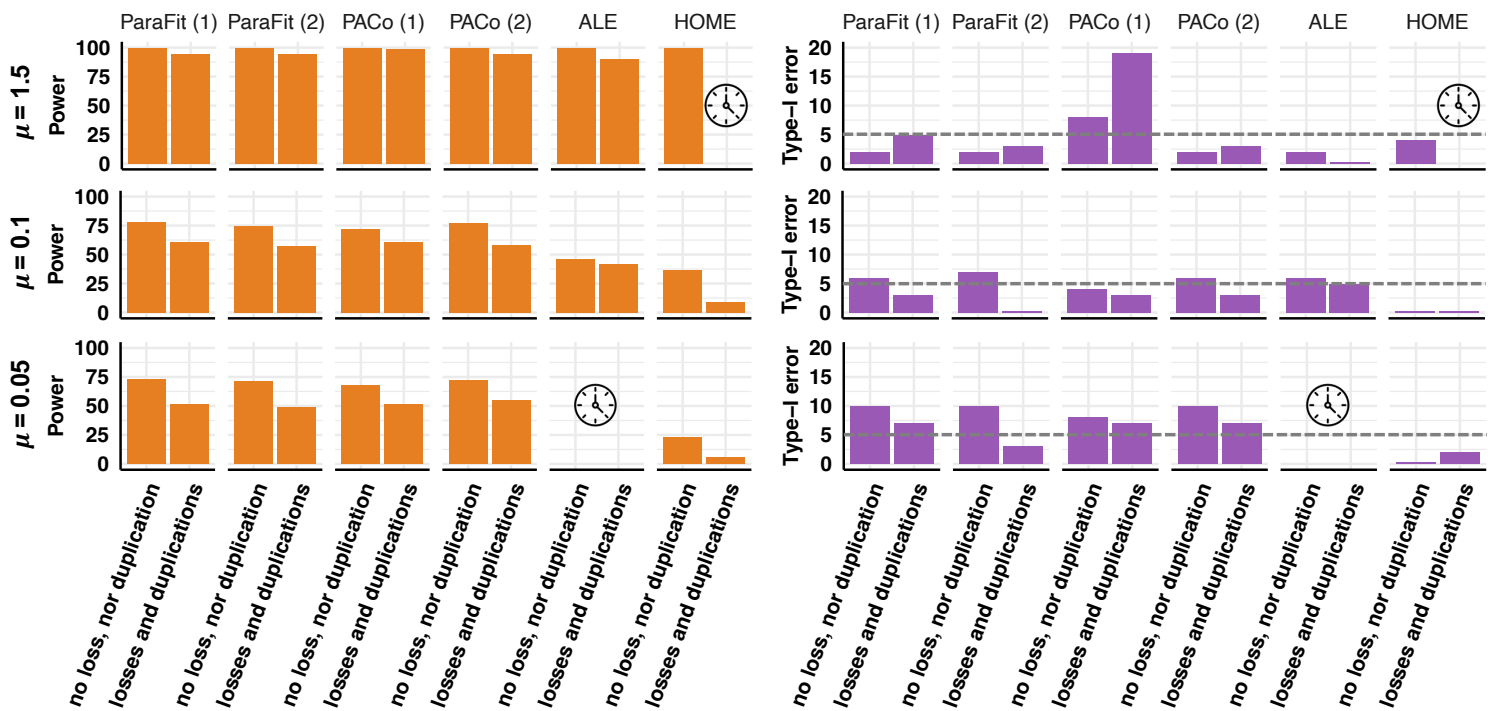


971

972 **Figure 2: Summary of the statistical performances of the different methods for**
 973 **detecting vertical transmission in host-associated microbiota:**

974 For each method, we indicated the statistical power (left) and the type-I error rate
 975 (right) for different substitution rates for the simulated microbial OTUs: $\mu=1.5$, $\mu=0.1$,
 976 and $\mu=0.05$. Statistical performances are reported for simulations without duplications
 977 or losses and simulations with both duplications and losses. The clock symbol
 978 indicates analyses that were too computationally intensive to be run in a reasonable
 979 amount of time and energy expense. Horizontal dashed grey lines indicate a 5% type-
 980 I error rate. Details on the statistical performances of the different approaches can be
 981 found in the supplements.

982

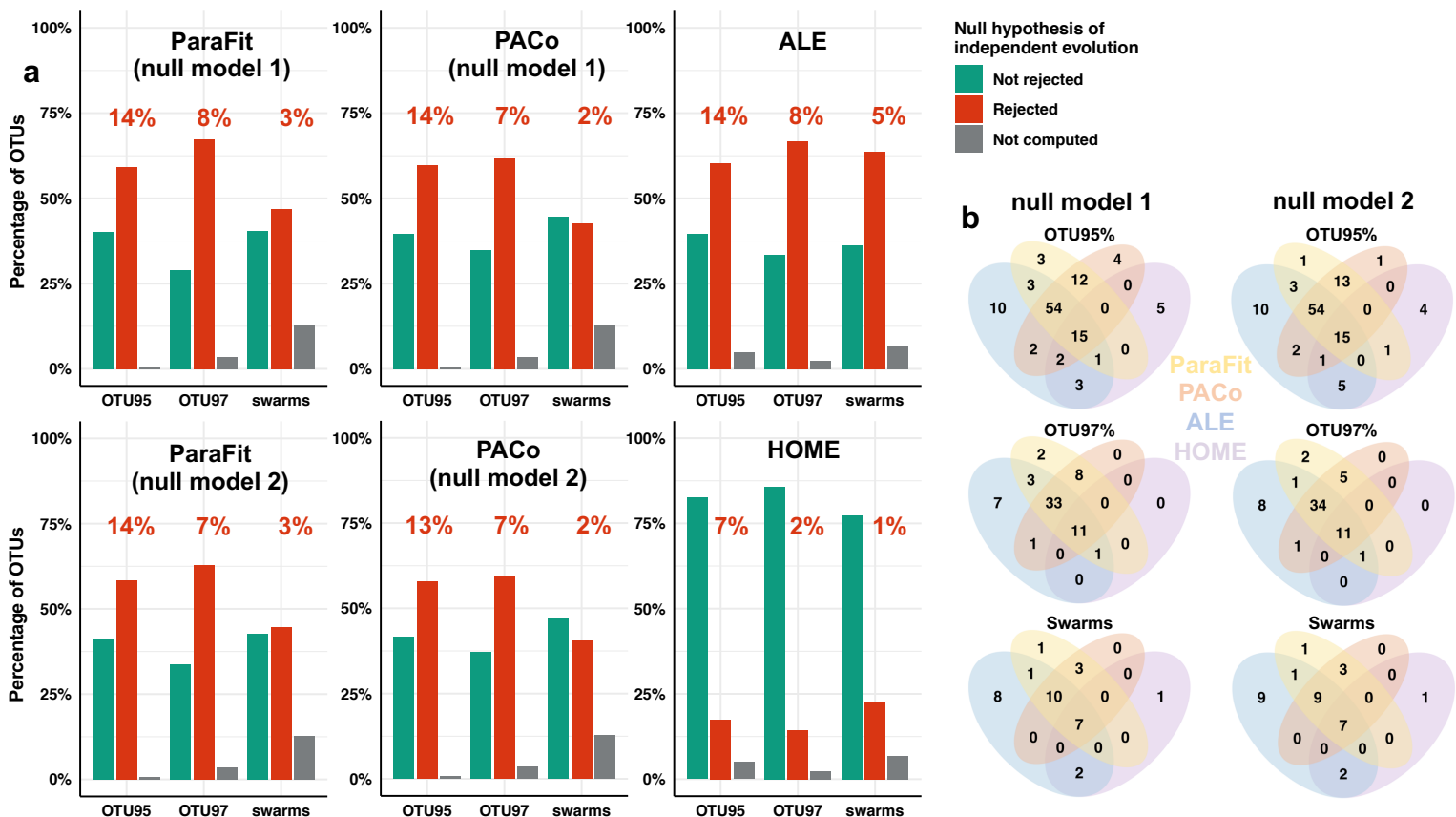


983 **Figure 3: Evidence for vertical transmission in primate gut microbiota varies**
 984 **according to the different methods used.**

985 (a) Percentage of core OTUs from the gut microbiota of primates rejecting (in red) or
 986 not (in green) the null hypothesis of independent evolution according to the different
 987 approaches tested: ParaFit (with null models 1 or 2), PACo (with null models 1 or 2),
 988 ALE, or HOME. OTUs colored in red thus represent vertically transmitted OTUs.
 989 Percentages at the top of each bar indicate the percentage of reads corresponding to
 990 these vertically transmitted OTUs in the whole primate gut microbiota. OTUs were
 991 clustered using the 95% or 97% similarity threshold or as Swarm OTUs.

992 (b) Venn diagrams indicating the number of OTUs that are simultaneously inferred to
 993 be vertically transmitted using the different approaches.

994

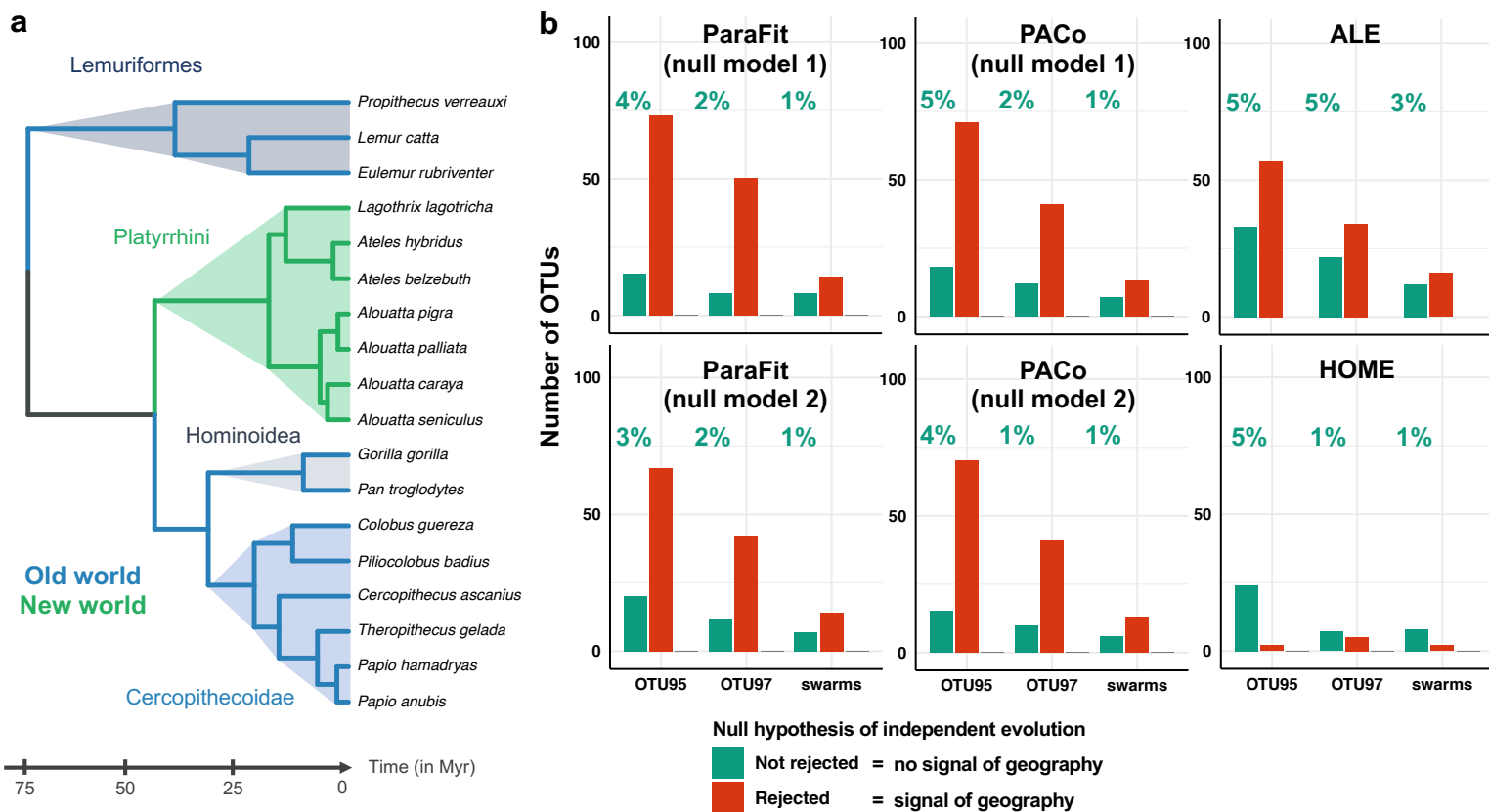


995

996 **Figure 4: Geography-driven cophylogeny:**

997 (a) Phylogenetic tree of the 18 primates with branches colored according to their native
 998 geographic area (the New or Old World).

999 (b) Number of OTUs, within those inferred to be vertically transmitted according to
 1000 ParaFit (with null models 1 or 2), PACo (with null models 1 or 2), ALE, or HOME, that
 1001 reject (in red) or not (in green) the hypothesis of independent evolution after
 1002 randomizing the associations between primate species and OTU strains within the Old
 1003 and New Worlds. If the cophylogenetic pattern is still significant (in red), the original
 1004 cophylogenetic signal is at least in part driven by geography (i.e. heterogeneous
 1005 environment pools of bacteria). If the cophylogenetic pattern is no longer significant
 1006 (in green), the original cophylogenetic signal arises from vertical transmissions (or
 1007 other, non-geographic effects). At the top of each bar, we indicated the percentage of
 1008 reads corresponding to these vertically transmitted OTUs in the whole primate gut
 1009 microbiota.



1010